Ultrasonics 99 (2019) 105961

Contents lists available at ScienceDirect

Ultrasonics

journal homepage: www.elsevier.com/locate/ultras

Excitation and detection of evanescent acoustic waves in piezoelectric plates: Theoretical and 2D FEM modeling

Iren Kuznetsova[a,*], Ilya Nedospasov[a], Andrey Smirnov[a], Zheng-hua Qian[b,*], Bin Wang[b], Xiao-yun Dai[b]

[a] Kotel'nikov Institute of Radio Engineering and Electronics of RAS, Moscow 125009, Russia
[b] State Key Laboratory of Mechanics and Control of Mechanical Structures/College of Aerospace Engineering, Nanjing University of Aeronautics and Astronautics, Nanjing 210016, China

A R T I C L E I N F O

Keywords:
Evanescent waves
Backward waves
Piezoelectric plates
Interdigital transducers
ZGV point

A B S T R A C T

This paper presents the results of the theoretical and 2D FEM modeling excitation and detection of evanescent acoustic waves in piezoelectric plates. By application of 2D ordinary differential equations derived by Auld, we obtained the dispersion curves of A_1 and SH_1 waves in YX $LiNbO_3$ and YX $KNbO_3$ plates in proximity to a zero group velocity point. The branches corresponding to evanescent acoustic waves are distinguished. A frequency range where real part of evanescent wave velocity is more than imaginary one was found. In this region evanescent mode is characterized by opposite directions of the phase and group velocities, i.e. this is backward wave. The theoretical analysis was verified in commercial 2D FEM software COMSOL 5.3. By modeling a set of interdigital transducers placed on the surface of Y-cut $LiNbO_3$ wafer with various values of the spatial period we found the resonant frequencies corresponding to evanescent A_1 mode. Due to proximity of this wave to a zero group velocity point its properties should be extremely sensitive to change of waveguide quality and ambient air. This is open the possibility to use these waves for development of high sensitive sensors and for nondestructive waveguide analysis.

1. Introduction

As is known, the acoustic waves in a plate are divided into antisymmetric (A_n) and symmetric (S_n) Lamb waves and waves with shear horizontal polarization (SH_n) [1]. For Lamb wave propagation the particles of a plate oscillate in the sagittal plane and for shear waves they oscillate in the plane of a plate perpendicular to the direction of wave propagation. These waves are characterized by the real wave numbers. The possibility of existence the acoustic waves with purely imaginary or complex wave numbers is known from literature. There are so-called evanescent or non-propagating waves [1–3]. In the case of a purely imaginary wave number, or when the imaginary part of the wave number significantly exceeds its real part, the evanescent mode corresponds to vibration near the source of an external force, decaying exponentially with distance from the source and does not transfer energy [1–4]. The dispersion curves for such wave types in the isotropic plates were plotted [1–4]. In Ref. [5] shear-horizontal waves with purely imaginary wave numbers propagating in the piezoelectric plates with cubic symmetry were theoretically investigated. Recently, the results of the theoretical study of the evanescent Lamb waves propagating in functionally graded piezoelectric-piezomagnetic plates have been published [6]. Mainly, nondissipated media characterized by zero viscosity were investigated. The dispersion curves for non-propagating waves in viscoelastic anisotropic plates, cylinders and multilayered structures were obtained by using a spectral collocation method in Ref. [7]. The characteristics of non-propagating Lamb waves in the bilayered viscoelastic structures were also theoretically investigated in Ref. [8]. There are also studies of the spectrum of the acoustic modes in structures containing dissipative media [9–11]. It was shown that the waveguide modes with the real and complex wave numbers in plates, tubes, cylindrical shells, at immersing into a liquid become bound [10–12]. It should be noted that the influence of liquid is very similar to the case of the presence of viscosity in the material [13] and, in this case, waves, even with a complex wave number, are always propagating.

Recently, the papers devoted to the theoretical and experimental study of the reflection of Lamb waves from the edge of a plate have appeared. Such reflection is accompanied by excitation including evanescent waves, which exist solely near the edge of the plate [1,14–20]. The existence of evanescent Lamb waves has been experimentally

* Corresponding authors.
E-mail addresses: kuziren@yandex.ru (I. Kuznetsova), qianzh@nuaa.edu.cn (Z.-h. Qian).

https://doi.org/10.1016/j.ultras.2019.105961
Received 26 March 2019; Received in revised form 8 July 2019; Accepted 9 July 2019
Available online 10 July 2019

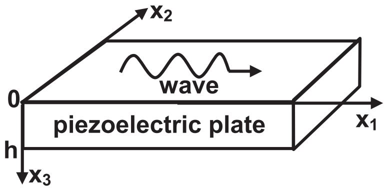

Fig. 1. Geometry of the problem.

proven at free-edge boundaries [21,22] and the possibility of their use for fatigue crack visualization has been confirmed in [23]. Interest in the study of such waves is attributed with the possibility of their use in nondestructive testing [24]. These waves also could be useful for development of a planar acoustic transducer for near field acoustic communication [25]. Moreover, due to the proximity of these waves to a cutoff frequency, they must be very sensitive to changes in the properties of an environment. This feature suggests the possibility of creating on their basis highly sensitive chemical acoustoelectronic sensors.

In this study, we present the results of theoretical analysis of the characteristics of evanescent waves and the peculiarities of their existence. A numerical simulation was performed to find the complex velocities of the SH_1 and A_1 acoustic waves in YX $KNbO_3$ and YX $LiNbO_3$ plates, respectively, then a 2D FEM analysis was performed with COMSOL 5.3 software.

2. Theoretical analysis

For theoretical analysis of acoustic wave propagation in a piezoelectric plate (Fig. 1) we used standard motion equation (1), Laplace's equation (2), and constitutive equations (3) for piezoelectric medium [26–29]:

$$\rho \partial^2 U_i/\partial t^2 = \partial T_{ij}/\partial x_j, \tag{1}$$

$$\partial D_j/\partial x_j = 0 \tag{2}$$

$$T_{ij} = C_{ijkl}\partial U_l/\partial x_k + e_{kij}\partial \Phi/\partial x_k, \quad D_j = -\varepsilon_{jk}\partial \Phi/\partial x_k + e_{jlk}\partial U_l/\partial x_k \tag{3}$$

Here U_i is the component of the mechanical displacement of the particles, t is the time, T_{ij} is the component of the mechanical stress, x_j is the coordinate, D_j is the component of the electrical displacement, Φ is the electrical potential, ρ, C_{ijkl},e_{ikl}, and ε_{jk} are the density, elastic, piezoelectric, and dielectric constants, respectively. The indices i, j, k, l = 1 ÷ 3 are space coordinate differentiation. The repeated indices in the subscript imply summation with respect to that index.

In the regions $x_3 < 0$ and $x_3 > h$ we used Laplace's equation for vacuum:

$$\partial D_j^{vac}/\partial x_j = 0. \tag{4}$$

The corresponding constitutive equation for vacuum has the follow form:

$$D_j^{vac} = -\varepsilon_0 \partial \Phi^{vac}/\partial x_j. \tag{5}$$

Here index *vac* denotes the values referred to the vacuum and ε_0 is the vacuum permittivity.

On the planes $x_3 = 0$ and $x_3 = h$ we used the next mechanical and electrical boundary conditions [26–29]:

$$T_{3j} = 0,\ \Phi^{vac} = \Phi;\ D_3^{vac} = D_3. \tag{6}$$

The general solution of the equations system (1)–(5) is sought as the sum of the plane inhomogeneous partial waves.

$$Y_\alpha(x_1, x_3, t) = Y_\alpha(x_3)\exp[j\omega(t - x_1/V)]. \tag{7}$$

Here, $\alpha = 1 \div 8$ for the piezoelectric plate and $\alpha = 1, 2$ for the vacuum; V is the complex wave velocity, ω is the angular wave frequency. We introduced the following normalized values [30,31]:

$$Y_\beta = \omega C_{11}^* U_\beta/V;\ Y_4 = T_{13}; Y_5 = T_{23};\ Y_6 = T_{33};\ Y_7 = \omega e^* \Phi/V_{ph};\ Y_8 = e^* D_3/\varepsilon_{11}^*, \tag{8}$$

where $\beta = 1, 2, 3$; C_{11}^*, ε_{11}^* are the normalizing material constants of the piezoelectric medium in the crystal-physical coordinate system; $e^* = 1$ [C/m^2].

The systems of eight and two 2D ordinary differential equations for the piezoelectric medium and vacuum, respectively, were obtained by the substitution of Eq. (7) in the Eqs. (1)–(5). Each of these systems can be presented as:

$$[A][dY/dx_3] = [B][Y]. \tag{9}$$

Here $[dY/dx_3]$ and $[Y]$ are 8D and 2D vectors for a piezoelectric medium and vacuum, respectively. Their components are determined in accordance with the expressions (8). The matrices $[A]$ and $[B]$ are square with the dimension of 8×8 for piezoelectric medium and one of 2×2 for vacuum. Because the matrix $[A]$ is singular ($\det[A] \neq 0$) one can write for each medium $[dY/dx_3] = [A^{-1}][B][Y] = [C][Y]$.

Further, to solve the system of Eq. (9), it is necessary to find the eigenvalues $\gamma^{(\alpha)}$ of the matrix $[C]$ and corresponding eigenvectors $[Y^{(\alpha)}]$, which determine the parameters of the partial waves for each medium. The general solution is a linear combination of all partial waves for each medium:

$$Y_p = \sum_{\alpha=1}^{N} A_\alpha Y_p^{(\alpha)} \exp(\gamma^{(\alpha)} x_3)\exp(i\omega[t - x_1/V]), \tag{10}$$

where the numbers of the eigenvalues N and the numbers of the normalized values p are equal 8 for piezoelectric medium and 2 for vacuum, respectively, A_α are unknown values. For the determination of the values A_α and complex wave velocity V we used the equations for mechanical and electrical boundary conditions (6), which were presented in the normalized form with considering Eq. (8). For a vacuum located in the regions $x_3 < 0$ and $x_3 > 0$, the eigenvalues with a negative and positive real part, respectively, are excluded from the consideration, since all variables in vacuum must have a decreasing amplitude when removed from a piezoelectric plate.

Thus, the unknown quantities A_α and velocity V can be determined from a system of the 10 homogeneous algebraic linear equations (6).

We used Visual Fortran software for draw up of own corresponding program. As a result, we found the complex wave velocity and distribution of amplitudes of the mechanical and electrical variables along plate thickness. Earlier the acoustic waves of higher order in YX $LiNbO_3$ and YX $KNbO_3$ plates were theoretically investigated [28,32]. The dispersion curves corresponding to forward and backward A_1 and SH_1 acoustic waves in YX $LiNbO_3$ and YX $KNbO_3$ plates, respectively, were plotted. In the present study, we carefully analyzed these dispersion curves in a region near a point of zero group velocity (ZGV). The material constants of $LiNbO_3$ and $KNbO_3$ were taken from [33,34].

As the result of the calculations, we found branches characterized by a complex velocity corresponding to the evanescent SH_1(E) and A_1(E) acoustic waves (Fig. 2). The analysis has shown that the wave vector of these waves is complex even in the absence of dissipation. The absolute value of the imaginary part of the velocity of these waves increases sharply with decrease parameter hf (h = plate thickness, f = wave frequency). In this case, the definition of the group velocity of these waves is not possible. As for the value of the phase velocity of such waves, it is necessary to use the next expression [35]:

$$V_{ph} = (V_R^2 + V_I)^2/V_R. \tag{11}$$

Here V_R and V_I are the real and imaginary parts of the complex wave velocity of the considered wave, respectively.

To define are these waves have backward or forward nature we used the effect that was described in [31]. It was shown that the phase velocity of forward waves is decreased and for backward waves it is increased under the electrical shorting a plate surface. The analysis of the evanescent waves SH_1(E) and A_1(E) (Fig. 2) have shown that their

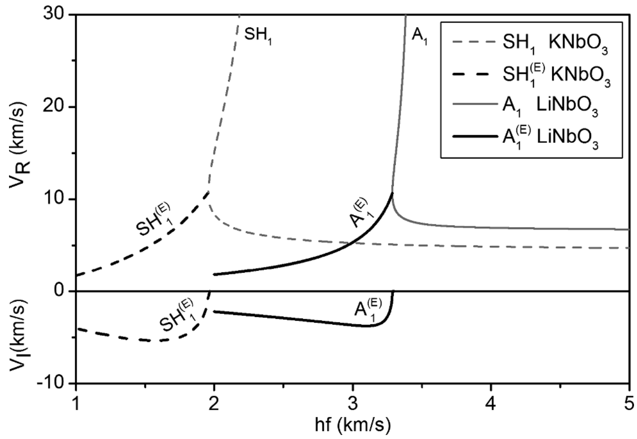

Fig. 2. Dependencies of the real and imaginary parts of the complex wave velocities vs parameter hf for SH_1 wave in YX $KNbO_3$ plate and for A_1 wave in YX $LiNbO_3$ plate.

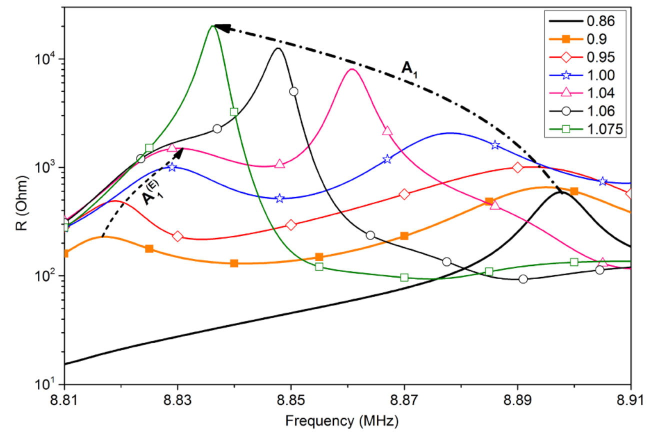

Fig. 4. Frequency dependencies of the real part of the impedance of IDTs for wavelengths 0.86 mm, 0.9 mm, 0.95 mm, 1 mm, 1.04 mm, 1.06 mm, and 1.075 mm placed on YX $LiNbO_3$ wafer. The arrows show the moving corresponding maximum.

phase velocity is increased under metallization of the plate surface, consequently, these waves have backward nature. From the quality consideration, it is possible to conclude that the presence such waves are possible only due to existence of the backward waves into spectrum. In this case, the evanescent mode is the only possible way for indissoluble continuation of the spectrum through a ZGV point.

The frequency range characterized by $V_R > V_I$ is wider for $KNbO_3$ than for $LiNbO_3$ as shown in Fig. 2. Most likely, this is related to higher piezoactivity of the waves in $KNbO_3$ [36–38].

3. Verification of excitation and detection of evanescent waves via 2D FEM analysis

The FEM commercial software COMSOL 5.3 was used to confirm the possibility of excitation and detection of the considered evanescent waves. The earlier method suggested based on use of the set of IDTs with various spatial periods has been presented in [30]. The set of IDTs for wavelengths λ in the range of 0.86–1.075 mm consisting of 7 pairs of Al strips placed on YX $LiNbO_3$ plate has been used for modeling. The thickness of the plate and IDT's fingers were 370 µm and 5 µm, respectively. The geometry of the IDTs and the net used in the simulation are shown in Fig. 3. On the edges of the plate, perfectly matched layers (PMLs) are located to prevent the reflections of the excited waves. Width of PML was equal 0.5 mm. It is assumed that these absorbing layers are characterized by a quadratic frequency dependence of the attenuation. It also assumed that the plate regions outside of the IDT are mechanically free, i.e. the mechanical stresses are equal to zero. In the area of the contact of IDT fingers with the plate, the mechanical continuities of the normal components of the mechanical displacements and mechanical stresses between the finger and the plate were used as the mechanical boundary conditions. The excitation of an acoustic wave was modeled by applying a variable electrical potential to the IDT's fingers (Fig. 3). In the model, the IDT was represented by a set of equipotential rectangles, and the region under the electrodes was divided into the small elements. The linear size of these elements was equal to λ/50 as shown in Fig. 3.

As a result of the simulation, the frequency dependencies of the real part of the electrical impedance of the IDT for different values of their spatial period λ/2 were obtained (Fig. 4).

The moving maxima corresponding to forward A_1 and backward evanescent $A_1(E)$ waves in YX $LiNbO_3$ plate are shown by arrows in Fig. 4. It can be seen that the evanescent mode exists in a limited frequency range and the branches A_1 (E) and A_1 merge into one near the ZGV point.

Fig. 5 shows 2D modes shape for $A_1(E)$ wave at cutoff and ZGV frequencies in agreement with Fig. 4.

4. Conclusion

The dispersion curves of A_1 and SH_1 acoustic waves in YX $LiNbO_3$ and YX $KNbO_3$ plates in the region near the ZGV point is theoretically studied. The branches corresponding to evanescent modes have been distinguished. It has been found that more piezoactive materials

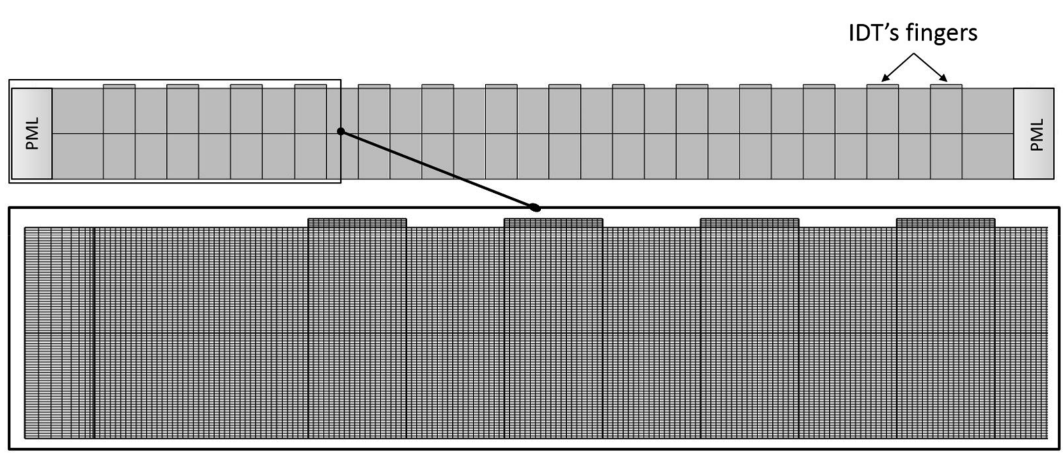

Fig. 3. Topology of the FEM model and corresponding net mesh.

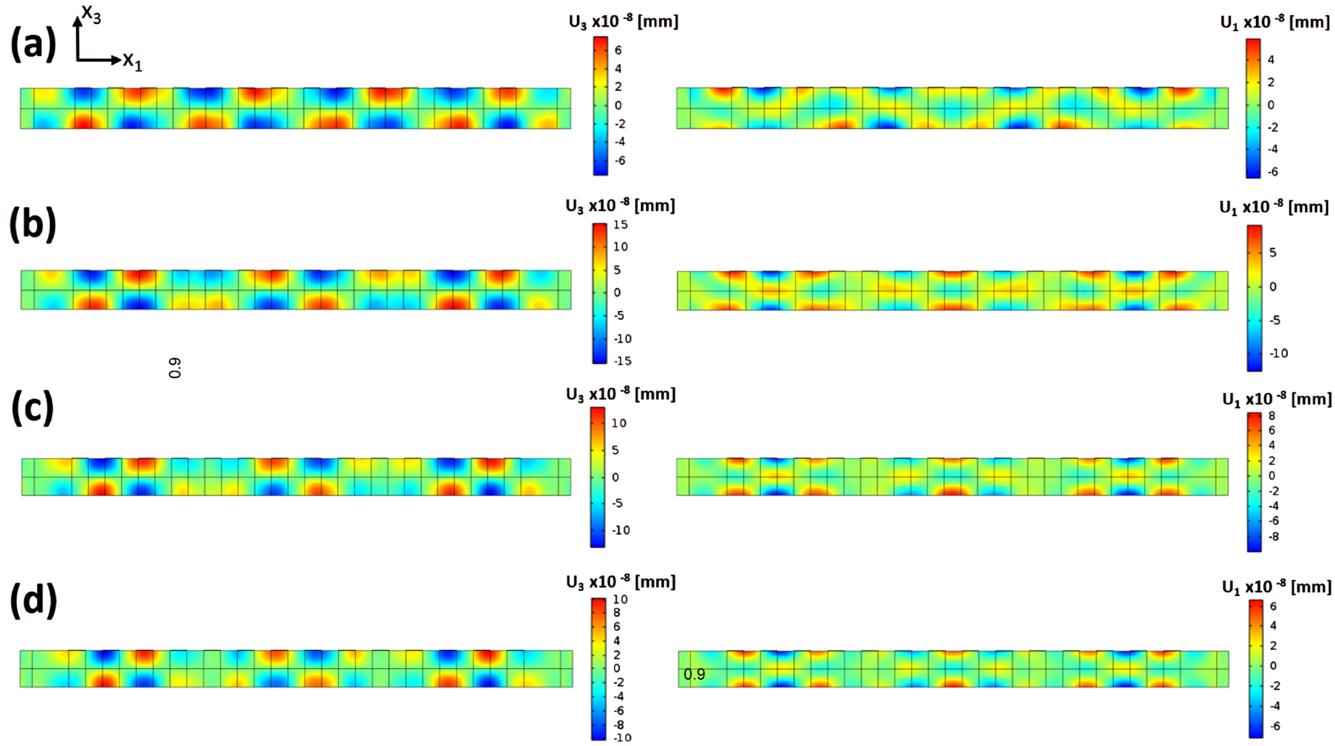

Fig. 5. 2D modes shape for A_1(E) wave in agreement with Fig. 4. The distributions of the displacements U_3 and U_1 are presented in left and right columns, respectively. The wavelength and hf are (a) 0.9 mm and 3.3064 km/s, (b) 0.95 mm and 3.3071 km/s, (c) 1 mm and 3.3109 km/s, (d) 1.04 mm and 3.3116 km/s.

characterized by more wide frequency range where evanescent modes could be detected. The possibility to excite and detect evanescent modes by the method based on a set of IDTs with various spatial periods was demonstrated and verified by FEM commercial software COMSOL 5.3. Due to proximity of evanescent waves to a ZGV point its properties should be extremely sensitive to change of waveguide quality and ambient air. Our results have theoretical significance for development of high sensitive sensors based on the evanescent waves and for non-destructive waveguide analysis.

Acknowledgements

This work is partially supported by government task of Kotelnikov IRE RAS in frame of approach to sensor development, Russian Foundation of Basic Research grants #19-07-00145-a in frame of acoustoelectronic device modeling via Comsol, #19-07-00070-a in frame of backward acoustic waves investigation, #17-07-00750-a in frame of acoustic wave analysis, the National Natural Science Foundation of China grants #11502108, #11611530686.

References

[1] B.A. Auld, Acoustic Fields and Waves in Solids vol. 2, John Wiley & Sons, New York, USA, 1973.
[2] R.H. Lyon, Response of an elastic plate to localized driving forces, J. Acoust. Soc. Am. 27 (2) (1955) 259–265.
[3] V. Pagneux, A. Maurel, Determination of Lamb mode eigenvalues, J. Acoust. Soc. Am. 110 (3) (2001) 1307–1314.
[4] R.D. Mindlin, J. Yang, An Introduction to the Mathematical Theory of Vibrations of Elastic Plates, World Scientific Publishing, New York, USA, 2006.
[5] H. Chen, J. Wang, J. Du, J. Yang, Propagation of shear-horizontal waves in piezoelectric plates of cubic crystals, Arch. Appl. Mech. 86 (3) (2016) 517–528.
[6] X. Zhang, Z. Li, J. Yu, The computation of complex dispersion and properties of evanescent Lamb wave in functionally graded piezoelectric-piezomagnetic plates, Materials 11 (2018) 1186.
[7] F.H. Quintanilla, M.J.S. Lowe, R.V. Craster, Full 3D dispersion curve solutions for guided waves in generally anisotropic media, J. Sound Vib. 363 (2016) 545–559.
[8] F. Simonetti, M.J.S. Lowe, On the meaning of Lamb mode evanescent branches, J. Acoust. Soc. Am. 118 (1) (2005) 186–192.
[9] R.D. Fay, O.V. Fortier, Transmission of sound through steel plates immersed in water, J. Acoust. Soc. Am. 23 (3) (1951) 339–346.
[10] S.I. Rokhlin, D.E. Chimenti, A.H. Nayfeh, On the topology of the complex wave spectrum in a fluid-coupled elastic layer, J. Acoust. Soc. Am. 85 (3) (1989) 1074–1080.
[11] F.D. Philippe, D. Clorennec, M. Ces, R. Anankine, C. Prada, Analysis of backward waves and quasi-resonance of shells with the invariants of the time reversal operator, Proceedings of Meetings on Acoustics ICA2013 vol.19, (2013) #1, 055022.
[12] G. Kaduchak, D.H. Hughes, P.L. Marston, Enhancement of the backscattering of high frequency tone bursts by thin spherical shells associated with a backwards wave: observations and ray approximation, J. Acoust. Soc. Am. 96 (6) (1994) 3704–3714.
[13] I.A. Nedospasov, V.G. Mozhaev, I.E. Kuznetsova, Unusual energy properties of leaky backward Lamb waves in a submerged plate, Ultrasonics 77 (2017) 95–99.
[14] P.J. Torvik, Reflection of wave trains in semi-infinite plates, J. Acoust. Soc. Am. 41 (2) (1967) 346–353.
[15] Y. Cho, J. Rose, A boundary element solution for a mode conversion study on the edge reflection of Lamb waves, J. Acoust. Soc. Am. 99 (1996) 2097–2109.
[16] R.D. Gregory, I. Gladwell, The reflection of a symmetric Rayleigh-Lamb wave at the fixed or free edge of a plate, J. Elast. 13 (2) (1983) 185–206.
[17] E. Le Clezio, M. Predoi, M. Castaings, B. Hosten, M. Rousseau, Numerical predictions and experiments on the free-plate edge mode, Ultrasonics 41 (2003) 25–40.
[18] S. Santhanam, R. Demirli, Reflection of Lamb waves obliquely incident on the free edge of a plate, Ultrasonics 53 (1) (2013) 271–282.
[19] M. Ratassepp, A. Klauson, F. Chati, Application of orthogonality-relation for the separation of Lamb modes at a plate edge: numerical and experimental predictions, Ultrasonics 57 (2015) 90–95.
[20] X. Yan, F.G. Yuan, A semi-analytical approach for SH guided wave mode conversion from evanescent into propagating, Ultrasonics 84 (2018) 430–437.
[21] O. Diligent, M.J.S. Lowe, E. Le Clezio, M. Castaings, B. Hosten, Prediction and measurement of evanescent Lamb modes at the free end of a plate when the fundamental antisymmetric mode A0 is incident, J. Acoust. Soc. Am. 113 (6) (2003) 3032–3042.
[22] M. Cès, D. Clorennec, D. Royer, C. Prada, Edge resonance and zero group velocity Lamb modes in a free elastic plate, J. Acoust. Soc. Am. 130 (2) (2011) 689–694.
[23] Y.K. An, H. Sohn, Visualization of non-propagating Lamb wave modes for fatigue crack evaluation, J. Appl. Phys. 117 (11) (2015) 114904.
[24] P. Cawley, D. Alleyne, The use of Lamb waves for the long range inspection of large structures, Ultrasonics 34 (2-5) (1996) 287–290.
[25] A. Fujii, N. Wakatsuki, K. Mizutani, A planar acoustic transducer for near field acoustic communication using evanescent wave, Jpn. J. Appl. Phys. 53 (2014) 07KB07.
[26] G. Farnell, Properties of elastic surface waves, Phys. Acoust. 50 (1970) 139–202. Academic Press: New York, USA.
[27] A.A. Oliner (Ed.), Acoustic Surface Waves, Springer, New York, USA, 1978.
[28] I.E. Kuznetsova, B.D. Zaitsev, I.A. Borodina, A.A. Teplykh, V.V. Shurygin,

S.G. Joshi, Investigation of acoustic waves of higher order propagating in plates of lithium niobate, Ultrasonics 42 (2004) 373–376.
[29] I.E. Kuznetsova, B.D. Zaitsev, S.G. Joshi, A.A. Teplykh, Effect of a liquid on the characteristics of antisymmetric Lamb waves in thin piezoelectric plates, Acoust. Phys. 53 (5) (2007) 537–563.
[30] B. Zaitsev, I. Kuznetsova, I. Nedospasov, A. Smirnov, A. Semyonov, New approach to detection of guided waves with negative group velocity: modeling and experiment, J. Sound Vib. 442 (2019) 155–166.
[31] I.E. Kuznetsova, I.A. Nedospasov, V.V. Kolesov, Z. Qian, B. Wang, F. Zhu, Influence of electrical boundary conditions on profiles of acoustic field and electric potential of shear-horizontal acoustic waves in potassium niobate plates, Ultrasonics 86 (2018) 6–13.
[32] B.D. Zaitsev, I.E. Kuznetsova, I.A. Borodina, A.A. Teplykh, The peculiarities of propagation of the backward acoustic waves in piezoelectric plates, IEEE Trans. Ultrason. Ferroelectr. Control 55 (7) (2008) 1660–1664.
[33] www.bostonpiezooptics.com/lithium-niobate.
[34] M. Zgonik, R. Schlesser, I. Biaggio, E. Voit, J. Tscherry, P. Gunter, Materials constants of KNbO3 relevant for electro- and acousto-optics, J. Appl. Phys. 74 (2) (1993) 1287–1297.
[35] M. Levy, H. Bass, R. Stern, Modern Acoustical Techniques for the Measurement of Mechanical Properties vol. 39, Academic Press, 2001.
[36] B.D. Zaitsev, I.E. Kuznetsova, I.A. Borodina, S.G. Joshi, Characteristics of acoustic plate waves in potassium niobate (KNbO3) single crystal, Ultrasonics 39 (1) (2001) 51–55.
[37] K. Yamanouchi, H. Odagawa, T. Kojima, T. Matsumura, Theoretical and experimental study of super high electromechanical coupling surface acoustic wave propagation in $KNbO_3$ single crystal, Electron. Lett. 33 (3) (1997) 193–194.
[38] K. Nakamura, M. Oshiki, H. Kitazume, SH-mode SAW and its acousto-optic interaction in $KNbO_3$, Proceddings of IEEE International Ultrasonics Symposium, 1988, pp. 1305–1308.